A generalized eigenvalue solution to the flutter stability problem with true damping: The p-L method

David Quero, Pierre Vuillemin, Charles Poussot-Vassal

▶ **To cite this version:**

David Quero, Pierre Vuillemin, Charles Poussot-Vassal. A generalized eigenvalue solution to the flutter stability problem with true damping: The p-L method. Journal of Fluids and Structures, 2021, 103, pp.103266. 10.1016/j.jfluidstructs.2021.103266 . hal-03201726

HAL Id: hal-03201726
https://hal.science/hal-03201726

Submitted on 19 Apr 2021

HAL is a multi-disciplinary open access archive for the deposit and dissemination of scientific research documents, whether they are published or not. The documents may come from teaching and research institutions in France or abroad, or from public or private research centers.

L'archive ouverte pluridisciplinaire **HAL**, est destinée au dépôt et à la diffusion de documents scientifiques de niveau recherche, publiés ou non, émanant des établissements d'enseignement et de recherche français ou étrangers, des laboratoires publics ou privés.

A generalized eigenvalue solution to the flutter stability problem with true damping: the p-L method

David Quero[a], Pierre Vuillemin[b], Charles Poussot-Vassal[b]

[a] *DLR (German Aerospace Center), Institute of Aeroelasticity, Göttingen, Germany*
[b] *ONERA / DTIS, Université de Toulouse, Toulouse, France*

Abstract

An alternative solution to the flutter equation with a true damping representation is presented. The p-L method transforms the nonlinear eigenvalue problem into a linear generalized eigenvalue formulation by interpolating the nonlinear aerodynamic term with help of the Loewner and shifted-Loewner matrices, avoiding any kind of approximation. Subsequently an equivalent generalized state-space formulation in the time-domain is obtained, which stability can be determined by solving a standard generalized eigenvalue problem. The proposed method is shown to describe the aerodynamic term throughout the complex plane by analytic continuation of the interpolating rational functions over the imaginary axis, whereas expansions based on polynomial basis functions have a limited validity for excursions outside it. Further, the p-L method matches the generalized aeroelastic analysis method (GAAM) framework representing true damping but requiring only samples of the aerodynamic term along the imaginary axis, avoiding additional computations for the aerodynamic term. Unlike methods which solve the nonlinear eigenvalue problem whereby some roots of the flutter equation may be missed, the p-L method is able to find all roots at once. The method is applied to well-known flutter benchmark cases from the literature, namely, several two-dimensional flutter cases and the AGARD 445.6 wing aeroelastic benchmark case.

1. Introduction

The determination of the stability boundaries of an aeroelastic system is one of the main topics within the aeroelasticity discipline. For a vehicle flying in the atmosphere it must be shown that the interaction between inertial, elastic and aerodynamic forces do not result in an unstable phenomenon (Anon., 2018). Flutter is the result of one of these possible instabilities and can be modeled by a linear (or linearized) aeroelastic system around a equilibrium condition. Even if the nonlinear aeroelastic system is under consideration, in light of Lyapunov's indirect theorem (Khalil and Grizzle, 2002) and if the aeroelastic system is at a equilibrium condition (this excludes dynamic stable conditions such as limit cycle oscillations) the nonlinear system is locally asymptotically stable if the linearized system around this condition is asymptotically stable. The analysis of the stability of linearized systems is thus of capital importance in order to ensure the stability of the aeroelastic system under consideration, which for the flutter problem can be then be determined by the roots of the flutter equation, see Section 3.

Due to the nature of the flutter equation, several assumptions have been made prior to obtaining its solution. There are two main difficulties that need to be addressed, namely, the nonlinear dependency of the aerodynamic term with the complex Laplace variable and the existence of aerodynamic solvers designed solely for the solution over the imaginary axis. Indeed and due to the property of analytic continuation (excluding exceptional points and curves in the form of

poles, other singularities, and branch cuts of the complex function (Carrier et al., 2005)) this should not be a restriction, as the complex function may be reconstructed from its values over the imaginary axis. On the one hand and due to the nonlinear aerodynamic term, the solution to the flutter solution has to be found by applying iterative techniques, typically the method of successive approximations, iteration on the determinant (Hassig, 1971) or nonlinear algebraic solvers solvers (Cardani and Mantegazza, 1978). As observed by Van Zyl (2001), the commonly used method of successive approximations may encounter convergence problems so that some roots of the flutter equation may not be found. In order to overcome this limitation, Chen (2000) and Van Zyl (2001) used a sweeping technique on the reduced frequency variable in order to obtain all the roots. This requires the repeated solution of a standard eigenvalue problem, even for conditions where the flutter equation is not satisfied. The present p-L method overcomes the difficulty caused by the presence of the nonlinear aerodynamic term by transforming it into a generalized state-space form through an inverse Laplace transform. Thus, at the expense of an increase in the size of the system matrices, all roots are obtained by solving once a standard generalized eigenvalue problem. Still the solution is found to be much faster in comparison to previous methods.

On the other hand, the limitation due to the availability of the aerodynamic term over the imaginary axis has led to the well-known p-k method of Hassig (1971) (or the extensively used modification of Rodden in order to include an aerodynamic damping matrix obtaining non-constant real coefficients for the nonlinear eigenvalue problem (Rodden et al., 1979)), by which the aerodynamic term is approximated by the value at the imaginary axis throughout the complex plane. This is valid when the real part of the roots of the flutter equation are very small. The g method further extends the region of validity compared to the p-k method by using a first-order Taylor series approximation of the aerodynamic damping term when moving away from the imaginary axis (Chen, 2000). Note that the order of the approximation can be increased by considering additional terms in the Taylor series expansion and higher-order methods such as the g^2 method have been presented (Ju and Qi, 2009). In Section 2.2 the limited ability of polynomial expansion methods when moving further away from the imaginary axis is shown. In that case, there is no guarantee that the Taylor series approximations perform better than the more simplistic p-k method.

The generalized aeroelastic analysis method (GAAM) presented by Edwards and Wieseman (2008) considers a true aerodynamic representation over the complex plane by extending existing aerodynamic solvers to the complex Laplace variable. A further modification of the GAAM formulation in order to obtain a nonlinear eigenvalue problem with (non-constant) real coefficients is given by Haddadpour and Firouz-Abadi (2009). Both works ((Edwards and Wieseman, 2008, Haddadpour and Firouz-Abadi, 2009)) use a potential-flow doublet-lattice method (DLM) (Albano and Rodden, 1969) solver as a function of the (nondimensional) complex Laplace variable.

Different than the previous techniques, the so-called p method aims at obtaining a true description of the aerodynamic term by applying a rational function approximation to the nonlinear term and using analytic continuation to represent it in the complex plane (Burkhart, 1977, Abel, 1979, Rodden and Bellinger, 1982, Karpel, 1982). Even though rational basis functions are suited for the analytic continuation of complex functions, the errors introduced by the approximation on the imaginary axis is translated into errors in the complex plane. The p-L method presented here combines the advantages of both the GAAM and p methods by truly interpolating the aerodynamic term and thus suppressing the error introduced by the p method and achieving a true representation as for the GAAM method, but reducing the computational time required for the computation of the aerodynamic term, as only the imaginary axis has to be considered. The p-L method overcome limitations of other existing methods at the only extend of increasing the size of the matrices considered. However, by transforming the nonlinear eigenvalue problem into a gener-

alized one, the p-L method is shown to be computationally more efficient in all cases analyzed in Section 4 when compared to previous methods for determining the roots of the flutter equation.

Regarding the structure of this work, Section 2 focuses on the representation of the aerodynamic term. The interpolation of the generalized aerodynamic forces (GAF) matrix within the Loewner framework is presented. A discussion on the suitability of rational interpolants versus polynomial basis for the representation of the GAF matrix outside the imaginary axis is presented, showing specific results for the generalized Theodorsen function in the Laplace domain. Once the transformation of the aerodynamic term into a generalized state-space form by interpolating the available sample points in the frequency domain, the resulting model is coupled with the structural dynamic model in Section 3, wherein a discussion on available methods for the solution of the flutter equation is presented and the advantages of the proposed p-L method are highlighted. In Section 4 several flutter benchmark cases are considered, showing the ability of the p-L method on truly representing truly the damping together with the advantages won from solving a standard eigenvalue problem instead of a nonlinear one. Finally, in Section 5 conclusions are drawn.

2. From aerodynamic frequency samples to the complex domain

In this section the aerodynamic term, which in general depends non-linearly on the Laplace variable s, is transformed to a generalized state-space form by interpolating the aerodynamic transfer function matrix over the imaginary axis and extending it by means of analytic continuation to the complex domain. It is common within the aerodynamic discipline to consider the nondimensional Laplace variable $p = s\,(L_{ref}/U_\infty) = g + ik$, with g the real part and $k = \omega\,(L_{ref}/U_\infty)$ the imaginary part equivalent to the reduced frequency, where L_{ref} is a reference length and U_∞ the true airspeed.

For the flutter equation (see Section 3) the aerodynamic term represented by the generalized aerodynamic forces (GAF) matrix $\mathbf{Q}_{hh}\,(p, M_\infty, Re_\infty, \mathbf{W}_0)$, as the roots of the flutter equation and not the aerodynamic load distribution over the airframe is of interest. M_∞ represents the Mach number, Re_∞ the Reynolds number and $\mathbf{W}_0$ the steady or equilibrium flow condition. Note that the Reynolds number dependency is only present when aerodynamic methods which model flow viscous effects are considered. Also, some common aerodynamic potential methods such as the doublet-lattice method (DLM) (Albano and Rodden, 1969) neglect the dependency on the steady flow condition $\mathbf{W}_0$. In the sequel the explicit dependency on the Mach number M_∞ is kept as $\mathbf{Q}_{hh}\,(p, M_\infty)$, as the aerodynamic methods used in Section 4 neglect the dependencies on Re_∞ and $\mathbf{W}_0$. For higher-fidelity aerodynamic methods considering these dependencies, the p-L method presented in this work is readily applicable and the dependency on M_∞ must be replaced by $(M_\infty, Re_\infty, \mathbf{W}_0)$.

As described in Section 1, the linearized aeroelastic problem around an equilibrium condition will be considered. This means that the aerodynamic term represented by the generalized aerodynamic forces (GAF) matrix $\mathbf{Q}_{hh}\,(p, M_\infty)$ depends linearly on the motion of the boundary surface at the body. For the flutter equation, the origin of the aerodynamic forces is the due solely to this motion and thus external perturbations, as for example induced by atmospheric turbulence, are not taken into account (see Section 3). For the actual system, an external perturbation will induce a motion of the boundary surface which may in turn trigger some instability if present.

As it will be seen in Section 3, the roots of the flutter equation (given by the solution of a nonlinear eigenvalue problem) are in general complex. As such, a representation of the aerodynamic term throughout the complex plane given by the Laplace variable p is required. Historically different methods have been developed in order to tackle this dependency. The p-k method (Hassig,

1971) approximates the aerodynamic term in the Laplace variable p by its corresponding value at the imaginary axis ik such that $\mathbf{Q}_{hh}(p, M_\infty) \approx \mathbf{Q}_{hh}(ik, M_\infty)$. Rodden et al. (1979) modified the p-k method of Hassig so that $\mathbf{Q}_{hh}(p, M_\infty) \approx \mathrm{Re}\{\mathbf{Q}_{hh}(ik, M_\infty)\} + \mathrm{Im}\{\mathbf{Q}_{hh}(ik, M_\infty)\}(p/k)$. In both variants the roots of the flutter equation are not exact when the real part is non-zero. Instead, the generalized aeroelastic analysis method (GAAM) method of Edwards and Wieseman (2008) properly considers the Laplace transform of the GAF term $\mathbf{Q}_{hh}(p, M_\infty)$, which usually requires the extension of aerodynamic solvers available in the frequency domain (Albano and Rodden, 1969, Thormann and Widhalm, 2013). It is important to note that the GAF term is obtained numerically (except for some specific cases where the analytical solution is known) and the consideration of additional values outside the imaginary axis is computationally more involved.

The p method tries to find an approximated Laplace transform of the GAF term $\mathbf{Q}_{hh}(ik, M_\infty)$ by approximating it first along the imaginary axis with a set of basis functions (usually rational functions) for which the Laplace transform is known. By means of analytic continuation (Carrier et al., 2005, Edwards et al., 1979, Stark, 1984), the term is extended afterwards over the complex plane by replacing ik by p. The success of the p method is directly linked to the quality of the approximation of the term $\mathbf{Q}_{hh}(ik, M_\infty)$ over the imaginary axis.

A compromise solution between the GAAM and p methods is found by the g method (Chen, 2000), where the complex GAF term $\mathbf{Q}_{hh}(ik, M_\infty)$ is extended for small values of g outside the imaginary axis by applying a Taylor series expansion and using the Cauchy-Riemann conditions:

$$\mathbf{Q}_{hh}(p, M_\infty) \approx \mathbf{Q}_{hh}(ik, M_\infty) + g\frac{d\mathbf{Q}_{hh}(ik, M_\infty)}{d(ik)}. \tag{1}$$

Higher-order versions of the g method have also been presented (Ju and Qi, 2009). For instance, the g^2 method uses a second-order Taylor series approximation:

$$\mathbf{Q}_{hh}(p, M_\infty) \approx \mathbf{Q}_{hh}(ik, M_\infty) + g\frac{d\mathbf{Q}_{hh}(ik, M_\infty)}{d(ik)} + \frac{1}{2}g^2\frac{d^2\mathbf{Q}_{hh}(ik, M_\infty)}{d(ik)^2}.$$

The terms corresponding to the derivatives of the GAF term with respect to the variable ik can be approximated by the use of finite differences. Central finite differences with a step $\triangle k = 10^{-4}$ are used in this work whenever the g or g^2 methods are used, see Sections 2.2 and 4.

However, as will become clear in Section 2.2, due to the limited properties of the analytic continuation offered by polynomial functions (Trefethen, 2019), these cannot be used for increasingly further excursions out of the imaginary axis. On the contrary, the rational interpolation is a suitable technique (Trefethen, 2019).

In order to avoid the solution of a nonlinear eigenvalue problem for the determination of the roots of the flutter equation and to increase the quality in the representation of the GAF term $\mathbf{Q}_{hh}(p, M_\infty)$, the p-L method interpolates the GAF term over the imaginary axis so that the well-behaved analytic continuation offered by rational functions can be effectively exploited throughout the complex plane. Note that within the p-L method and compared with the GAAM method, no additional computations of the aerodynamic solution are required for values $g \neq 0$. Unlike for the p method, the p-L method interpolates the GAF term avoiding any kind of approximation and as such the quality in the representation of the aerodynamic term is not compromised.

2.1. Tangential interpolation: the p-L method

The basis of the p-L method presented here is the interpolation of the aerodynamic term $\mathbf{Q}_{hh}(ik, M_\infty)$ over the imaginary axis, taking subsequent advantage of the well behavior offered

by the rational functions for the analytic continuation throughout the complex plane. In order to perform the interpolation over the imaginary axis ik, the Loewner framework is employed (Mayo and Antoulas, 2007). This technique has already been employed in the context of aeroservoelasticity by Quero et al. (2019) in order to remove the dependency of poles selection and possibly additional optimizations as in the classical context of rational approximation (Roger, 1977, Karpel, 1982, Morino et al., 1995, Pasinetti and Mantegazza, 1999, Ripepi and Mantegazza, 2013) when generating aeroservoelastic models. In this work the Loewner realization is used so as to transform the nonlinear eigenvalue problem for the determination of the roots of the flutter equation into a standard generalized eigenvalue problem, see Section 3. This requires the determination of a generalized state-space model which interpolates the data $\mathbf{Q}_{hh}\left(ik, M_\infty\right)$ as:

$$\begin{aligned} \mathbf{E}_a\left(M_\infty\right)\frac{d\mathbf{x}_a\left(t\right)}{dt} &= \left(\frac{U_\infty}{L_{ref}}\right)\mathbf{A}_a\left(M_\infty\right)\mathbf{x}_a\left(t\right)+\mathbf{B}_a\left(M_\infty\right)\mathbf{u}_h\left(t\right), \\ \mathbf{Q}_h\left(t, M_\infty\right) &= \left(\frac{U_\infty}{L_{ref}}\right)\mathbf{C}_a\left(M_\infty\right)\mathbf{x}_a\left(t\right), \end{aligned} \tag{2}$$

where $\mathbf{E}_a \in \mathbb{R}^{n_a \times n_a}$, $\mathbf{A}_a \in \mathbb{R}^{n_a \times n_a}$, $\mathbf{B}_a \in \mathbb{R}^{n_a \times n_a}$, and $\mathbf{C}_a \in \mathbb{R}^{n_h \times n_a}$ with the matrix $\mathbf{E}_a\left(M_\infty\right)$ in general singular. The input to the system is given by the vector of generalized coordinates $\mathbf{u}_h \in \mathbb{R}^{n_h}$ and the output by the vector of aerodynamic forces $\mathbf{Q}_h \in \mathbb{R}^{n_h}$ projected into the generalized coordinates, caused by the particular combination contained in the vector $\mathbf{u}_h$. By making use of the Loewner framework, the state vector $\mathbf{x}_a \in \mathbb{R}^{n_a}$ is of minimal order (Mayo and Antoulas, 2007) and contains n_a states. Note that the factor (U_∞/L_{ref}) multiplying the matrices $\mathbf{A}_a$ and $\mathbf{C}_a$ allows for the consideration of the reduced frequency k directly into the sample points required for the application of the Loewner framework. The corresponding transfer function matrix $\hat{\mathbf{Q}}_{hh}\left(p, M_\infty\right) \in \mathbb{C}^{n_h \times n_h}$ is given by:

$$\hat{\mathbf{Q}}_{hh}\left(p, M_\infty\right) = \mathbf{C}_a\left(M_\infty\right)\left(p\mathbf{E}_a\left(M_\infty\right)-\mathbf{A}_a\left(M_\infty\right)\right)^{-1}\mathbf{B}_a\left(M_\infty\right). \tag{3}$$

The aim is to compute the set of matrices $\left\{\mathbf{E}_a\left(M_\infty\right), \mathbf{A}_a\left(M_\infty\right), \mathbf{B}_a\left(M_\infty\right), \mathbf{C}_a\left(M_\infty\right)\right\}$ with the minimum number of required states n_a, which transfer function matrix $\hat{\mathbf{Q}}_{hh}\left(p, M_\infty\right)$ in Eq. 3 interpolates the transfer function $\mathbf{Q}_{hh}\left(p, M_\infty\right)$ at a finite set of n_p values $\left\{p_l, \mathbf{Q}_{hh}\left(p_l, M_\infty\right)\right\}$, $1 \leq l \leq n_p$, that is, $\hat{\mathbf{Q}}_{hh}\left(p_l, M_\infty\right) = \mathbf{Q}_{hh}\left(p_l, M_\infty\right)$ with $p_l = ik_l$. The method described by Mayo and Antoulas (2007) is briefly reviewed here.

First, the available data at the set $\{p_l\}$ is completed with the complex conjugate values (denoted by *):

$$\left\{p_l, \mathbf{Q}_{hh}\left(p_l, M_\infty\right)\right\} \cup \left\{-p_l, \mathbf{Q}^*_{hh}\left(p_l, M_\infty\right)\right\},$$

where a total number of n_s sample points is obtained. This set is then split into the left and right interpolatory sets $\left\{\mu_q\right\}, q = 1, ..., n_l$ and $\left\{\lambda_r\right\}, r = 1, ..., n_r$ such that $\{p_l\} \cup \{-p_l\} = \{\mu_q\} \cup \{\lambda_r\}$. The left and right sets contain the (n_l) odd and (n_r) even sample points respectively. This partition is carried out such that if the total number of sample points n_s is even, $n_l = n_r = n_s/2$. If n_s is odd then $n_l = n_r + 1 = (n_s + 1)/2$. Associated to the left and right sets the following interpolatory conditions are fulfilled by construction (Mayo and Antoulas, 2007):

$$\left\{\mu_q, \mathbf{l}_q, \mathbf{v}_q \mid \mu_q \in \mathbb{C}, \mathbf{l}_q, \mathbf{v}_q \in \mathbb{C}^{n_h}, \mathbf{v}_q^T = \mathbf{l}_q^T\mathbf{Q}_{hh}\left(\mu_r, M_\infty\right), \;\; q = 1, ..., n_l\right\},$$

$$\left\{\lambda_r, \mathbf{r}_r, \mathbf{w}_r \mid \lambda_r \in \mathbb{C}, \mathbf{r}_r, \mathbf{w}_r \in \mathbb{C}^{n_h}, \mathbf{w}_r = \mathbf{Q}_{hh}\left(\lambda_q, M_\infty\right)\mathbf{r}_r,\ \ r = 1, ..., n_r\right\}.$$

By expanding this (tangential) interpolatory conditions to matrices (Wang et al., 2010), the following conditions are fulfilled:

$$\left\{\mu_q, \mathbf{L}_q, \mathbf{V}_q \mid \mu_q \in \mathbb{C}, \mathbf{L}_q \in \mathbb{C}^{n_t \times n_h}, \mathbf{V}_q = \mathbf{L}_q\mathbf{Q}_{hh}\left(\mu_q, M_\infty\right) \in \mathbb{C}^{n_t \times n_h},\ \ q = 1, ..., n_l\right\},$$

$$\left\{\lambda_r, \mathbf{R}_r, \mathbf{W}_r \mid \lambda_r \in \mathbb{C}, \mathbf{R}_r \in \mathbb{C}^{n_h \times n_t}, \mathbf{W}_r = \mathbf{Q}_{hh}\left(\lambda_r, M_\infty\right)\mathbf{R}_r \in \mathbb{C}^{n_h \times n_t},\ \ r = 1, ..., n_r\right\}.$$

In the case considered here the transfer function matrix $\mathbf{Q}_{hh}\left(p, M_\infty\right)$ is squared and thus, by setting $n_t = n_h$ and choosing proper $\mathbf{L}_q$ and $\mathbf{R}_r$ satisfying the condition $\text{rank}\left(\mathbf{L}_q\right) = \text{rank}\left(\mathbf{R}_r\right) = n_h$, all entries of the transfer function matrix are exploited and the interpolation is exact. In this work the matrices $\mathbf{L}_r$ and $\mathbf{R}_q$ are chosen to be $\mathbf{I}_{n_h}$, the identity size of order n_h.

In order to obtain real generalized state-space matrices, the left and right interpolatory data can next be reordered into real (zero frequency) and complex conjugate pairs (for frequency values distinct from zero) (Ionita, 2013):

$$\left\{\mu_1, ..., \mu_{n_l}\right\} = \left\{\mu_1, ..., \mu_{n_{lr}}\right\} \cup \left\{\mu_1, \bar{\mu}_1, ..., \mu_{n_{lc}}, \bar{\mu}_{n_{lc}}\right\}, \tag{4}$$

$$\left\{\mathbf{L}_1, ..., \mathbf{L}_{n_l}\right\} = \left\{\mathbf{L}_1, ..., \mathbf{L}_{n_{lr}}\right\} \cup \left\{\mathbf{L}_1, \bar{\mathbf{L}}_1, ..., \mathbf{L}_{n_{lc}}, \bar{\mathbf{L}}_{n_{lc}}\right\},$$

$$\left\{\mathbf{V}_1, ..., \mathbf{V}_{n_l}\right\} = \left\{\mathbf{V}_1, ..., \mathbf{V}_{n_{lr}}\right\} \cup \left\{\mathbf{V}_1, \bar{\mathbf{V}}_1, ..., \mathbf{V}_{n_{lc}}, \bar{\mathbf{V}}_{n_{lc}}\right\},$$

where $n_{lr} + 2n_{lc} = n_l$ for the left interpolatory set and:

$$\left\{\lambda_1, ..., \lambda_{n_r}\right\} = \left\{\lambda_1, ..., \lambda_{n_{rr}}\right\} \cup \left\{\lambda_1, \bar{\lambda}_1, ..., \lambda_{n_{rc}}, \bar{\lambda}_{n_{rc}}\right\}, \tag{5}$$

$$\left\{\mathbf{R}_1, ..., \mathbf{R}_{n_r}\right\} = \left\{\mathbf{R}_1, ..., \mathbf{R}_{n_{rr}}\right\} \cup \left\{\mathbf{R}_1, \bar{\mathbf{R}}_1, ..., \mathbf{R}_{n_{rc}}, \bar{\mathbf{R}}_{n_{rc}}\right\},$$

$$\left\{\mathbf{W}_1, ..., \mathbf{W}_{n_r}\right\} = \left\{\mathbf{W}_1, ..., \mathbf{W}_{n_{rr}}\right\} \cup \left\{\mathbf{W}_1, \bar{\mathbf{W}}_1, ..., \mathbf{W}_{n_{rc}}, \bar{\mathbf{W}}_{n_{rc}}\right\},$$

with $n_{rr} + 2n_{rc} = n_r$ for the right interpolatory set. From these data the block-format Loewner $\mathbb{L}$ and shifted Loewner $\mathbb{L}_\sigma$ matrices $\mathbb{L}_\sigma$ are defined blockwise as (Mayo and Antoulas, 2007, Wang et al., 2010):

$$\mathbb{L}_{qr}\left(M_\infty\right) = \frac{\mathbf{V}_q\left(M_\infty\right)\mathbf{R}_r\left(M_\infty\right) - \mathbf{L}_q\left(M_\infty\right)\mathbf{W}_r\left(M_\infty\right)}{\mu_q - \lambda_r} \in \mathbb{C}^{n_h \times n_h},$$

$$\mathbb{L}_{\sigma,qr}\left(M_\infty\right) = \frac{\mu_q\mathbf{V}_q\left(M_\infty\right)\mathbf{R}_r\left(M_\infty\right) - \lambda_r\mathbf{L}_q\left(M_\infty\right)\mathbf{W}_r\left(M_\infty\right)}{\mu_q - \lambda_r} \in \mathbb{C}^{n_h \times n_h},$$

and satisfy two specific Sylvester equations (Mayo and Antoulas, 2007, Wang et al., 2010). Conveniently, they do not need to be solved as the generalized state-space matrices can be readily obtained from the Loewner $\mathbb{L} \in \mathbb{C}^{n_h n_l \times n_h n_r}$ and shifted Loewner $\mathbb{L}_\sigma \in \mathbb{C}^{n_h n_l \times n_h n_r}$ matrices, which contain the respective blocks $\mathbb{L}_{qr}$ and $\mathbb{L}_{\sigma,qr}$.

Upon the convenient ordering of the interpolatory data defined by Eqs. 4 and 5 a further transformation is required in order to obtain real matrices. This is achieved out by the use of the following transformation matrices:

$$\mathbf{T}_L = \begin{bmatrix} \mathbf{I}_{n_h n_{lr}} & \mathbf{0} & & \cdots & & \mathbf{0} \\ \mathbf{0} & \mathbf{T}_1 & \mathbf{0} & & & \\ & & \ddots & & & \vdots \\ \vdots & & \mathbf{0} & \mathbf{T}_{q_c} & \mathbf{0} & \\ & & & & \ddots & \mathbf{0} \\ \mathbf{0} & & \cdots & & \mathbf{0} & \mathbf{T}_{n_{lc}} \end{bmatrix}, \quad \mathbf{T}_{q_c} = \frac{1}{\sqrt{2}} \begin{bmatrix} \mathbf{I}_{n_h} & \mathbf{I}_{n_h} \\ -i\mathbf{I}_{n_h} & i\mathbf{I}_{n_h} \end{bmatrix}, \quad q_c = 1, ..., n_{lc},$$

$$\mathbf{T}_R = \begin{bmatrix} \mathbf{I}_{n_h n_{rr}} & \mathbf{0} & & \cdots & & \mathbf{0} \\ \mathbf{0} & \mathbf{T}_1 & \mathbf{0} & & & \\ & & \ddots & & & \vdots \\ \vdots & & \mathbf{0} & \mathbf{T}_{r_c} & \mathbf{0} & \\ & & & & \ddots & \mathbf{0} \\ \mathbf{0} & & \cdots & & \mathbf{0} & \mathbf{T}_{n_{rc}} \end{bmatrix}, \quad \mathbf{T}_{r_c} = \frac{1}{\sqrt{2}} \begin{bmatrix} \mathbf{I}_{n_h} & \mathbf{I}_{n_h} \\ -i\mathbf{I}_{n_h} & i\mathbf{I}_{n_h} \end{bmatrix}, \quad r_c = 1, ..., n_{rc},$$

where $\mathbf{I}$ refers to the identity matrix of size specified by the subscript. As explained in Mayo and Antoulas (2007), the rank of the Loewner pencil $x\mathbb{L} - \mathbb{L}_\sigma$ with $x \in \{\mu_q\} \cup \{\lambda_r\}$ contains the minimal McMillan degree of the interpolating model. Thus, considering the (economic) singular value decomposition (SVD) of the real matrices:

$$[\mathbf{T}_L \mathbb{L} \mathbf{T}_R^* \quad \mathbf{T}_L \mathbb{L}_\sigma \mathbf{T}_R^*] = \mathbf{Y}_L \mathbf{\Sigma}_L \mathbf{X}_L^T, \quad \begin{bmatrix} \mathbf{T}_L \mathbb{L} \mathbf{T}_R^* \\ \mathbf{T}_L \mathbb{L}_\sigma \mathbf{T}_R^* \end{bmatrix} = \mathbf{Y}_R \mathbf{\Sigma}_R \mathbf{X}_R^T, \tag{6}$$

the minimal order of the generalized state-space matrices is ensured. In practice, a numerical rank tolerance is required in order to retain the first r of singular values in $\mathbf{\Sigma}_L$ and $\mathbf{\Sigma}_R$. In this work a tolerance value of $\sigma_{Lr}/\sigma_{L,1} \geq \epsilon_r$ and $\sigma_{Rr}/\sigma_{R,1} \geq \epsilon_r$ with $\epsilon_r = 10^{-6}$ is imposed, so that the first $r = \max(Lr, Rr)$ singular values in both decompositions are kept, and where $\sigma_{L,1}$ and $\sigma_{R,1}$ denote the first singular values of the two SVD decompositions in Eq. 6 respectively.

Using the singular vectors of Eq. 6 as projectors the generalized state-space matrices are finally obtained:

$$\begin{aligned} &\mathbf{E}_a(M_\infty) = -\mathbf{Y}_L^T \mathbf{T}_L \mathbb{L}(M_\infty) \mathbf{T}_R^* \mathbf{X}_R, \ \mathbf{A}_a = -\mathbf{Y}_L^T \mathbf{T}_L \mathbb{L}_\sigma(M_\infty) \mathbf{T}_R^* \mathbf{X}_R, \\ &\mathbf{B}_a = \mathbf{Y}_L^T \mathbf{T}_L \mathbf{V}(M_\infty), \ \mathbf{C}_a(M_\infty) = \mathbf{W}(M_\infty) \mathbf{T}_R^* \mathbf{X}_R, \end{aligned} \tag{7}$$

which is a time-domain representation of the aerodynamic system with transfer function $\hat{\mathbf{Q}}_{hh}(p, M_\infty)$, see Eq. 3. Note that this representation is valid for the complex Laplace variable p and is not restricted to the imaginary axis ik. Depending on the aerodynamic theory used and the frequency range of interest $[k_{min}, k_{max}]$ where the sample points are contained, the matrix $\mathbf{E}_a$ may be singular. For instance, if the analytical two-dimensional unsteady incompressible flow containing the Theodorsen function is considered, two poles at infinity are present (Quero et al., 2019), which is connected to the singularity of the matrix $\mathbf{E}_a$. However, if the spatial domain is discretized within

the aerodynamic modeling approach and very high frequencies are considered, the resulting aerodynamic transfer functions will decay with increasing frequencies and may as well be represented by a proper transfer function, that is, the matrix $\mathbf{E}_a$ could be inverted. However, this "low-pass" filter introduced by the spatial discretization is not physical and additional states are required to describe the phenomenon, which in turn increase the size of the vector $\mathbf{x}_a$. Thus, a careful selection of the frequency range of interest is recommended. For the application cases of Section 4 a maximum value of the reduced frequency $k_{max} = 3$ has been considered. Note that unlike for aeroservoelastic models where a nonsingular matrix $\mathbf{E}_a$ is sought in order to avoid the use of differential-algebraic equations (DAE) solvers (Quero et al., 2019), no transformation of the generalized state-space into a common state-space with invertible $\mathbf{E}_a$ is required when determining the roots of the flutter equation, see Section 3.1. The presence of the matrix $\mathbf{E}_a$ in the representation of the aerodynamic system is ultimately responsible for the solution of a generalized eigenvalue problem within the *p-L* method.

If the model described by Eq. 2 were to be used for time-domain simulations and due to the fact that the Loewner realization is not stability preserving, additional considerations must be taken into account in order to enforce stability (Quero et al., 2019, Gosea et al., 2020). However, in the case of the flutter stability problem solely the roots related to the wind-off structural eigenvalues are of interest and with an additional mode tracking algorithm (see Section 3.1), no stability enforcement is required on the aerodynamic part and the interpolation of the aerodynamic transfer function remains exact.

2.2. Rational versus polynomial representation in the complex plane

In order to demonstrate the capabilities of the proposed *p-L* method in representing the true damping component g, an analytical case where the aerodynamic solution is known in the complex plane is chosen. The generalized Theodorsen function $C(p)$ has been considered by Edwards (Edwards, 1977, Edwards et al., 1979) and represents a generalization of the Theodorsen function typically computed on the imaginary axis, namely, as function of the reduced frequency k, which can be extended to a dependency on the nondimensional Laplace variable p:

$$C(p) = \frac{H_1^{(2)}(p)}{H_1^{(2)}(p) + iH_0^{(2)}(p)},$$

with H_0 and H_1 the Hankel functions of first and second kind (Theodorsen, 1935). For two-dimensional cases in incompressible flow the Theodorsen functions play the role of the GAF term, as both the lift and pitch moment coefficients can be readily obtained from it, see Sections 4.1, 4.1.1 and 4.1.2. The generalized Theodorsen function is defined throughout the complex plane $\mathbb{C}$ except for logarithmic branch points at the origin and at infinity. Also, a branch cut along the negative real axis makes them single valued (Edwards and Wieseman, 2008). More generally, Edwards and Wieseman (2008) generalized this concept to general GAF matrices $\mathbf{Q}_{hh}(p, M_\infty)$ obtained from different aerodynamic models. For instance, a DLM code was modified in order to compute the corresponding aerodynamic terms through the complex plane p by using the variables transformation $\hat{p} = k - ig$.

Figs. 1 and 2 show the real and imaginary parts of the Theodorsen function $C(ik)$ as function of the reduced frequency k, that is, over the imaginary axis. In this case all methods considered here, namely the *p-k*, the *g*, the proposed *p-L* and the GAAM methods, lead to the same values. Note that in this section the reference values are provided by the GAAM method, as it explicitly

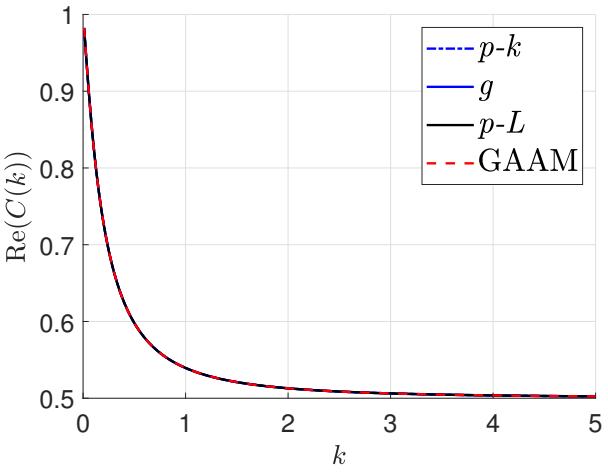

Figure 1: Real part of the generalized Theodorsen function on the imaginary axis.

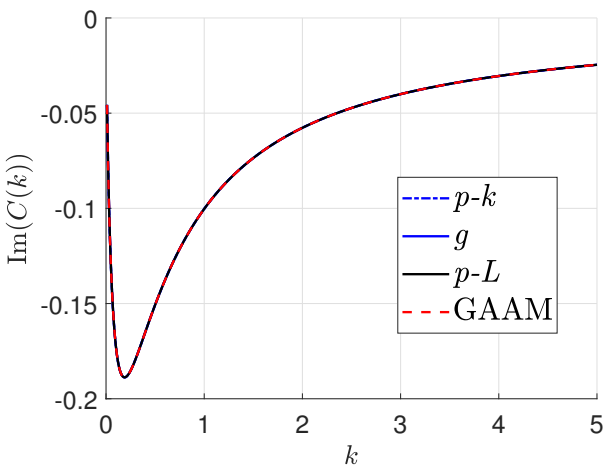

Figure 2: Imaginary part of the generalized Theodorsen function on the imaginary axis.

considers the dependency of the generalized Theodorsen function with the complex variable p. Results obtained by the p method have not been considered here, as they approximate the GAF term along the imaginary axis and as such the effect of the analytic continuation out of the imaginary axis cannot be judged independently of this approximation.

Figs. 3 and 4 represent the real and imaginary parts of the Theodorsen function versus the reduced frequency k but for a real part equal to $g = -0.02$. The aim here is to show the improvement of the g^2 method over the g method at a particular value of g. Also, the g method improves the prediction over the p-k method. Next it will become clear that the ability of the polynomial approximations (including the Taylor series) is limited for regions close to the imaginary axis and that the interpolation based on rational functions is able to properly extend the interpolation over the complex plane instead.

Polynomial approximation methods such as the g^2 method should be used carefully, as increasing the distance from the imaginary axis leads to an increasing mismatch with respect to the reference generalized Theodorsen function (labeled as GAAM), see Figs. 5 and 6. There, the real and imaginary parts of the generalized Theodorsen function $C(p)$ is shown for a constant angle $\theta = 90.005$ (deg) with respect to the real axis, $p = |p| e^{i\theta}$. Note that the value $\theta = 90$ (deg) corresponds to the Theodorsen function, that is, the values over the imaginary axis. This type of representation of the generalized Theodorsen function $C(p)$ for a constant angle θ have previously been used by Edwards (1977). It is clear from Figs. 5 and 6 that the g^2 method rapidly deteriorates when increasing the distance off the imaginary axis, and in that case, the g method provides a better representation when compared to the reference GAAM values. This is believed to be related to the ill-posedness of analytic continuation for polynomial basis functions, as even for higher-order polynomials offering a very precise interpolation in the axis of interest, the existence of the Bernstein ellipses limit the region of extension outside this axis (Trefethen, 2019, 2020). As stated by Trefethen (2019), "*in many applications a complex function can be analytically continued, in theory, to the rest of the complex plane, apart from exceptional points and curves in the form of poles, other singularities, and branch cuts. Computing such continuations numerically, however, is a difficult problem. One could try approximating the function by a polynomial, but this approach will be useless outside the largest Bernstein ellipse in which the function is analytic.*

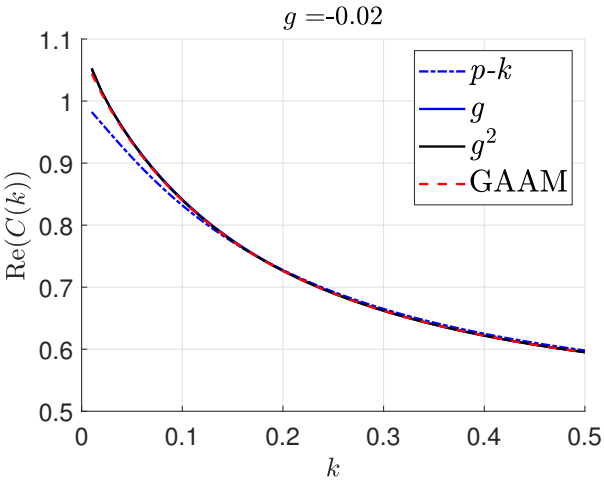

Figure 3: Real part of the generalized Theodorsen function for $g = -0.02$.

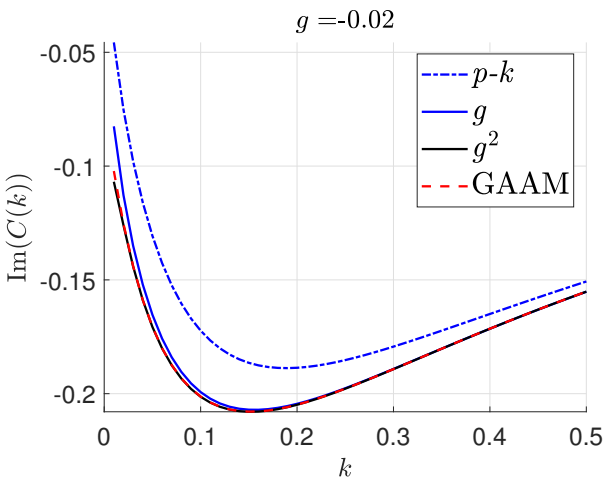

Figure 4: Imaginary part of the generalized Theodorsen function for $g = -0.02$.

Rational functions, by contrast, may be effective for continuation much further out."

In order to assess the results achieved by the proposed p-L method, a value of $\theta = 130$ (deg) is considered in Figs. 7 and 8. In this case the g^2 method is not shown due to the mismatch in several orders of magnitude with respect to the reference GAAM values. As expected, the g method notably improves the p-k prediction, which is in turn outperformed by the p-L method. Due to the nature of the p-L method based on rational interpolation, a truly representation model similar tothe GAAM method is achieved, including regions outside the imaginary axis.

3. Flutter equation

Now the aerodynamic and the structural dynamic models are coupled. The number n_g of degrees of freedom (dof) which describe the structural behavior is reduced after applying a modal truncation and retaining a number n_h of representative natural eigenmodes of the structure in the matrix $\boldsymbol{\phi}_0 \in \mathbb{R}^{n_g \times n_h}$, which are obtained as eigenvectors of the structure (wind-off conditions) with no damping. The resulting set of homogeneous (with no source term) ordinary differential equations (ODE), already projected into the corresponding set of generalized coordinates $\mathbf{u}_h$ after modal truncation, can be expressed as:

$$\mathbf{M}_{hh}\frac{d^2\mathbf{u}_h(t)}{dt^2} + \mathbf{B}_{hh}\frac{d\mathbf{u}_h(t)}{dt} + \mathbf{K}_{hh}\mathbf{u}_h(t) - q_{dyn}\int_0^t \mathbf{Q}_{hh}\left((t-\tau)\left(\frac{U_\infty}{L_{ref}}\right), M_\infty\right)\mathbf{u}_h(\tau) = \mathbf{0}, \quad (8)$$

where $\mathbf{M}_{hh} = \boldsymbol{\phi}_0^T\mathbf{M}_{gg}\boldsymbol{\phi}_0$, $\mathbf{B}_{hh} = \boldsymbol{\phi}_0^T\mathbf{B}_{gg}\boldsymbol{\phi}_0$ and $\mathbf{K}_{hh} = \boldsymbol{\phi}_0^T\mathbf{K}_{gg}\boldsymbol{\phi}_0$. Here, $(\mathbf{M}_{gg}, \mathbf{B}_{gg}, \mathbf{K}_{gg})$ and $(\mathbf{M}_{hh}, \mathbf{B}_{hh}, \mathbf{K}_{hh})$ represent the mass, damping and stiffness matrices in physical and generalized coordinates. The last term represent the motion-induced aerodynamic forces, with $q_{dyn} = \rho_\infty U_\infty^2/2$ denoting the dynamic pressure. The integral term corresponds to the Duhamel integral (Marques and Azevedo, 2008) and represents the aerodynamic response caused by an arbitrary motion by means of a convolution integral. There, $\mathbf{Q}_{hh}\left((t-\tau)\left(U_\infty/L_{ref}\right), M_\infty\right)$ is the matrix of impulse responses caused by the generalized coordinates $\mathbf{u}_h$. The factor (U_∞/L_{ref}) is considered so as to obtain a dependency with the nondimensional Laplace variable $p = sL_{ref}/U_\infty$ upon application

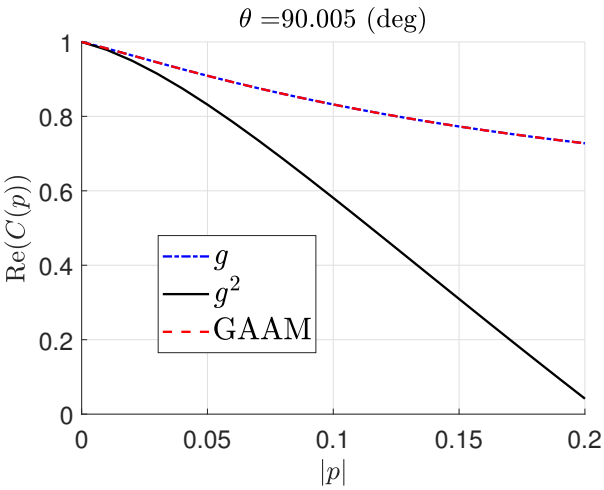

Figure 5: Real part of the generalized Theodorsen function for $\theta = 90.005$ (deg).

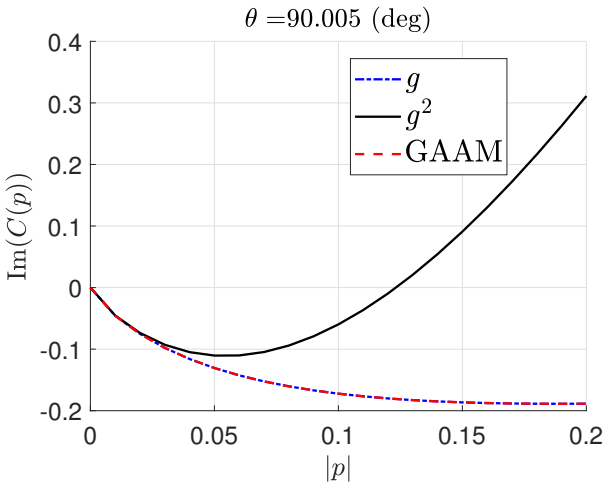

Figure 6: Imaginary part of the generalized Theodorsen function for $\theta = 90.005$ (deg).

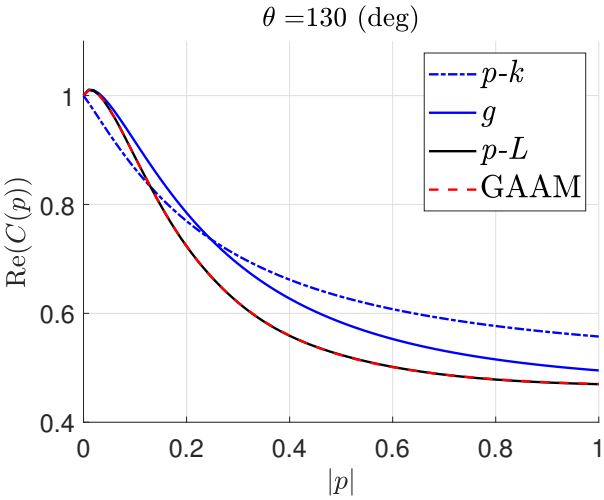

Figure 7: Real part of the generalized Theodorsen function for $\theta = 130$ (deg).

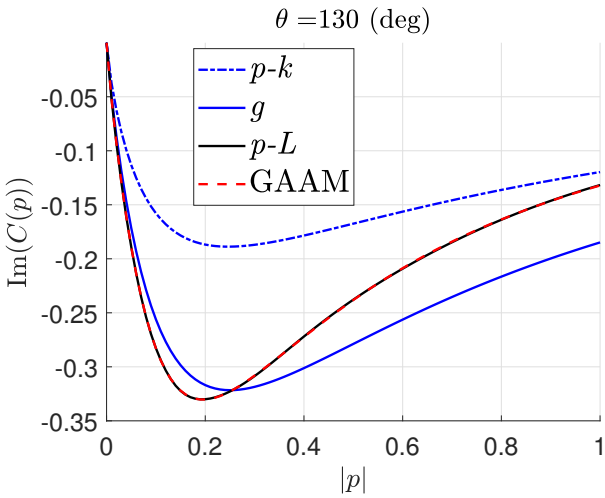

Figure 8: Imaginary part of the generalized Theodorsen function for $\theta = 130$ (deg).

of a Laplace transform. The dynamic pressure is linked to the Mach number M_∞ through the freestream density (ρ_∞) and velocity (U_∞) but it is usually handled as a parameter for a fixed value of the Mach number by either using standard atmospheric relations at a particular altitude value or by the conditions imposed in a wind tunnel. As described in Section 2, the dependency of the GAF matrix $\mathbf{Q}_{hh}$ with the Reynolds number Re_∞ and the steady flow condition (represented here with the general vector of flow variables $\mathbf{W}_0$) has been dropped in the sequel for the sake of clarity.

Instead of performing time-domain simulations to analyze the stability of Eq. 8, a Laplace transform which converts the problem into a (nonlinear) algebraic one:

$$\mathcal{L}\left\{\mathbf{f}\left(t\right)\right\} = \mathbf{f}\left(s\right) = \int_0^\infty \mathbf{f}\left(t\right) e^{-st} dt, \;\; s \in \mathbb{C}, \;\; \mathbf{f}\left(t\right) \in \mathbb{R}^{m \times n}, \;\; \mathbf{f}\left(s\right) \in \mathbb{C}^{m \times n},$$

resulting in the so-called flutter equation:

$$\left[p^2 \left(\frac{U_\infty}{L_{ref}}\right)^2 \mathbf{M}_{hh} + p\left(\frac{U_\infty}{L_{ref}}\right) \mathbf{B}_{hh} + \mathbf{K}_{hh} - q_{dyn} \mathbf{Q}_{hh}\left(p, M_\infty\right)\right] \mathbf{u}_h\left(p\right) = \mathbf{F}_{hh}\left(p, M_\infty\right) \mathbf{u}_h\left(p\right) = \mathbf{0}, \tag{9}$$

where $\mathcal{L}\left\{\mathbf{u}_h\left(t\right)\right\} = \mathbf{u}_h\left(s\right)$ and $\mathcal{L}\left\{\mathbf{Q}_{hh}\left(t\left(\frac{U_\infty}{L_{ref}}\right), M_\infty\right)\right\} = \mathbf{Q}_{hh}\left(p, M_\infty\right)$ and the nondimensional Laplace variable $p = sL_{ref}/U_\infty$ has been considered, so that the dependencies of $\mathbf{F}_{hh}$ and $\mathbf{u}_h$ with s and p can be interchanged. Note that the Laplace transform and not the Fourier transform has been chosen, as the solution of the homogeneous ODE with no source term and non-zero conditions is sought (Shinners, 1998). The GAF matrix $\mathbf{Q}_{hh}\left(p, M_\infty\right)$ corresponds to the Laplace transform of the impulse responses matrix $\mathbf{Q}_{hh}\left(t\left(\frac{U_\infty}{L_{ref}}\right), M_\infty\right)$. Eq. 9 represents a linearized condition (with respect to the generalized coordinates $\mathbf{u}_h$) around the equilibrium state which (global) stability, by virtue of Lyapunov's indirect theorem (Khalil and Grizzle, 2002), determines the local stability of a nonlinear system around the same equilibrium conditions.

For non-zero homogeneous solutions of Eq. 9 the determinant of $\mathbf{F}_{hh}\left(p, M_\infty\right)$ must be zero, $\det\left(\mathbf{F}_{hh}\left(p, M_\infty\right)\right) = 0$. This condition defines in general a nonlinear eigenvalue problem on the nondimensional Laplace variable p due to the dependence of the GAF matrix (p, M_∞), which can then be analyzed for a fixed U_∞ value and a sweep in the parameter q_{dyn}. Eigenvalues with a negative real part represent a stable condition, as the associated homogeneous response will decay for increasing times. The instability onset is thus defined at the condition where a root crosses the imaginary axis from the left-half complex plane, so that the real part becomes postive, indicating an increasing amplitude with time in the homogeneous response.

The GAAM method solves Eq. 9 in order to obtain the roots of $\det\left(\mathbf{F}_{hh}\left(p, M_\infty\right)\right) = 0$. As described in Section 2, the aerodynamic term $\mathbf{Q}_{hh}\left(p, M_\infty\right)$ is commonly obtained for harmonic motion of the generalized coordinates $\mathbf{u}_h$, that is, for values over the imaginary axis $\mathbf{Q}_{hh}\left(ik, M_\infty\right)$. Note that recently URANS aerodynamic solvers have been modified as to obtain the GAF matrix directly over the imaginary axis (Albano and Rodden, 1969, Thormann and Widhalm, 2013, Jacobson et al., 2020), suppressing the numerical dependency on the amplitude values when using the time-domain simulations, as for instance when establishing indicial responses (Marques and Azevedo, 2008). The *p-L* method of Section 3.1 can be readily applied to GAF matrices obtained from these solvers.

The nonlinear eigenvalue problem defined by Eq. 9 contains a quadratic nonlinear term given by $p^2\left(U_\infty/L_{ref}\right)^2 \mathbf{M}_{hh}$. This can be recast into the companion form:

$$[\mathbf{A}(p, M_\infty) - p\mathbf{I}] \begin{bmatrix} \mathbf{u}_h(p) \\ p\mathbf{u}_h(p) \end{bmatrix} \tag{10}$$

$$= \left(\begin{bmatrix} \mathbf{0} & \mathbf{I} \\ -\left(\frac{U_\infty}{L_{ref}}\right)^2 \mathbf{M}_{hh}^{-1}\left(\mathbf{K}_{hh} - q_{dyn}\mathbf{Q}_{hh}(p, M_\infty)\right) & -\left(\frac{L_{ref}}{U_\infty}\right)\mathbf{M}_{hh}^{-1}\mathbf{B}_{hh} \end{bmatrix} - p\mathbf{I} \right) \begin{bmatrix} \mathbf{u}_h(p) \\ p\mathbf{u}_h(p) \end{bmatrix} = \mathbf{0}$$

which represents a linear eigenvalue problem in the wind-off case, that is, with the aerodynamic term $q_{dyn}\mathbf{Q}_{hh}(p, M_\infty)$ set to zero. Eq. 10 is the companion form of the GAAM method, which can further be reformulated as to obtain real matrices (Haddadpour and Firouz-Abadi, 2009). Similarly, Rodden et al. (1979) further modified the p-k method of Hassig introducing a split between the real and imaginary parts of the GAF matrix $\mathbf{Q}_{hh}$ in order to obtain a quadratic eigenvalue problem with real matrices, which can in turn be recast into a companion form which represents a linear eigenvalue problem which must be solved at each fixed value of the reduced frequency k. Note that this is a companion form but not truly linearized, as the coefficients of the matrix $\mathbf{A}(p, M_\infty)$ (now real) are not constant as they depend on the reduced frequency k:

$$\mathbf{A}(p, M_\infty) = \begin{bmatrix} \mathbf{0} & \mathbf{I} \\ -\mathbf{A}_1(p, M_\infty) & -\mathbf{A}_2(p, M_\infty) \end{bmatrix}, \tag{11}$$

$$\mathbf{A}_1(p, M_\infty) = \left(\frac{U_\infty}{L_{ref}}\right)^2 \mathbf{M}_{hh}^{-1}\left(\mathbf{K}_{hh} - q_{dyn}\mathrm{Re}\left\{\mathbf{Q}_{hh}(ik, M_\infty)\right\}\right),$$

$$\mathbf{A}_2(p, M_\infty)\left(\frac{L_{ref}}{U_\infty}\right)\mathbf{M}_{hh}^{-1}\left[\mathbf{B}_{hh} - q_{dyn}\left(\frac{L_{ref}}{U_\infty}\right)\frac{\mathrm{Im}\left\{\mathbf{Q}_{hh}(ik, M_\infty)\right\}}{k}\right].$$

As a result of this reformulation, an additional aerodynamic damping matrix $-q_{dyn}\mathrm{Im}\left\{\mathbf{Q}_{hh}\right\}(g/k)$ has been added. With $\mathbf{A}(p, M_\infty)$ defined by Eq. 11, a total of $2n_h$ eigenvalues and their corresponding eigenvectors is computed for a fixed value of the reduced frequency k. However, the coefficients of the matrix premultiplying the eigenvector $\left[\mathbf{u}_h^T(p)\ \ p\mathbf{u}_h^T(p)\right]^T$ in Eq. 11 are non-constant and thus, additional eigenvalues such as those responsible for divergence may appear for the aeroelastic problem (Edwards and Wieseman, 2008), see Sections 3.1 and 4.1.2. An equivalent companion form has also been presented for the g method (Chen, 2000).

Independent of the formulation of the flutter equation, either in the form of Eq. 9 or in the companion form of Eq. 10, several techniques are available for the determination of the roots of the flutter equation:

- Regula Falsi (false position method) iteration on Eq. 9 (Hassig, 1971), where the iteration is carried out on the determinant of $\mathbf{F}_{hh}$ using a Regula Falsi (false position method) iteration.
- Method of successive approximations, where at each iteration a linear eigenvalue problem is solved. The iteration progresses defined by matching the imaginary part of the Laplace variable p with the reduced frequency k until a particular convergence is achieved. However, the method of successive iterations may miss some roots if some specific conditions are not met (Van Zyl, 2001).
- Application of a sweeping technique. Pitt (1999) applied a non-iterative p-k method by sweeping on the circular frequency ω and interpolating the roots to the flutter solution so

as to avoid the expensive interpolation of the GAF matrix. Chen (2000) applied a sweeping technique in the reduced frequency k to a companion form for the g method. Similarly, Van Zyl (2001) also applied an iterative technique on the reduced frequency k in order to find all roots to the flutter equation in the form of Eq. 9, as some of them may be missed by the method of successive approximations. A flutter solution based on a sweep on the reduced frequency is also implemented in Nastran in the companion form of Eq. 11 for the p-k method and is denoted as the *PKS* method (MSC.Software, 2011). By applying a sweeping technique, the iterative solution of the nonlinear eigenvalue problem is replaced by a series of linear eigenvalue problems, which have to be computed also at conditions for which the flutter equation does not hold.

- Solution by a nonlinear algebraic solver. In this case the eigenvector $\mathbf{u}_h$ is obtained simultaneously with the eigenvalue p, and thus an additional condition in order to fix the size of the eigenvector is applied (Cardani and Mantegazza, 1978, Bindolino and Mantegazza, 1987). Upon splitting the real and imaginary parts, the resulting system of nonlinear equations is given by:

$$\begin{aligned} \begin{bmatrix} \mathrm{Re}\left\{\mathbf{F}_{hh}\left(p, M_\infty\right)\right\} & \mathrm{Im}\left\{\mathbf{F}_{hh}\left(p, M_\infty\right)\right\} \\ \text{-}\mathrm{Im}\left\{\mathbf{F}_{hh}\left(p, M_\infty\right)\right\} & \mathrm{Re}\left\{\mathbf{F}_{hh}\left(p, M_\infty\right)\right\} \end{bmatrix} \begin{bmatrix} \mathrm{Re}\left\{\mathbf{u}_h\right\} \\ \mathrm{Im}\left\{\mathbf{u}_h\right\} \end{bmatrix} &= \begin{bmatrix} \mathbf{0} \\ \mathbf{0} \end{bmatrix}, \\ \mathrm{Re}\left\{\mathbf{u}_h^T \mathbf{c} \mathbf{u}_h\right\} &= 1, \\ \mathrm{Im}\left\{\mathbf{u}_h^T \mathbf{c} \mathbf{u}_h\right\} &= 0, \end{aligned} \tag{12}$$

with $\mathbf{c}$ a constant weighting matrix. The number of unknowns and equations is $2n_h + 2$ and a different solution must be obtained for each aeroelastic root, which is found by setting proper initial values to the nonlinear solver. Thus, the nonlinear system is at least solved n_h times. Note that in order to find divergence roots specific initial conditions over the real axis should be used in order to find additional eigenvalues (Edwards and Wieseman, 2008).

In Section 4, all results obtained for the the p-k, g or GAAM methods have been obtained by applying a nonlinear algebraic solver (Powell, 1968) to Eq. 12. There, a different condition for the normalization of the eigenvectors has been used, $\mathrm{Re}\left\{\max\left(|\mathbf{u}_h|\right)\right\} = \max\left(\boldsymbol{\phi}_0 \mathbf{e}_j\right)$ and $\mathrm{Im}\left\{\max\left(|\mathbf{u}_h|\right)\right\} = 0$, where the vector $\mathbf{e}_j \in \mathbb{R}^{n_h}$ selects the corresponding column to the mode j. Note that compared to this solution technique, the proposed p-L method avoids the solution of a nonlinear eigenvalue problem, as explained in Section 3.1.

Unlike the methods which focus on solving the nonlinear eigenvalue problem, either directly in the form of Eq. 9, the companion form of Eq. 10 or in the nonlinear algebraic formulation of Eq. 12, the p method builds an aeroelastic state-space model from which stability behavior can be deduced from the real part of its eigenvalues. Typically this aeroelastic state-space has made use of different rational function approximations (RFA) techniques which approximate the aerodynamic transfer function over the imaginary axis (Roger, 1977, Karpel, 1982, Morino et al., 1995, Pasinetti and Mantegazza, 1999, Ripepi and Mantegazza, 2013). By means of an inverse Fourier transform, known for rational functions, a state-space form valid for arbitrary motions of the generalize coordinates $\mathbf{u}_h$ is obtained. The particular form of the resulting state-space formulation depends on which RFA is chosen and includes an additional number of n_a states which represent the aerodynamic term, resulting in a total of $2n_h + n_a$ states. The p method relies on the good properties of analytic continuation of rational functions in order to represent the aerodynamic term throughout the complex plane. However, the approximation error due to the fit

on the data over the imaginary axis is inherently present on the extension into the complex plane. The *p-L* method presented in Section 3.1 is similar to the *p* method in the sense that a state-space is obtained, from which the flutter stability can be readily obtained. A main advantage of the *p-L* method is that the aerodynamic term is interpolated instead and thus approximation errors, as introduced by RFA techniques, are removed.

3.1. Generalized eigenvalue solution with true damping: the p-L method

Considering now Eq. 2 a generalized state-space model of first-order in time in the augmented state variable $\mathbf{x}_{ae} = [\mathbf{u}_h^T \ \frac{d\mathbf{u}_h^T}{dt} \ \mathbf{x}_a^T]^T$ is obtained for the aeroelastic system:

$$\begin{bmatrix} \mathbf{I} & \mathbf{0} & \mathbf{0} \\ \mathbf{0} & \mathbf{I} & \mathbf{0} \\ \mathbf{0} & \mathbf{0} & \mathbf{E}_a(M_\infty) \end{bmatrix} \frac{d}{dt}\left(\begin{bmatrix} \mathbf{u}_h \\ \frac{d\mathbf{u}_h}{dt} \\ \mathbf{x}_a \end{bmatrix}\right) = \begin{bmatrix} \mathbf{I} & \mathbf{0} & \mathbf{0} \\ -\mathbf{M}_{hh}^{-1}\mathbf{K}_{hh} & -\mathbf{M}_{hh}^{-1}\mathbf{B}_{hh} & \mathbf{M}_{hh}^{-1}q_{dyn}\mathbf{C}_a(M_\infty) \\ \mathbf{B}_a(M_\infty) & \mathbf{0} & \mathbf{A}_a(M_\infty) \end{bmatrix} \begin{bmatrix} \mathbf{u}_h \\ \frac{d\mathbf{u}_h}{dt} \\ \mathbf{x}_a \end{bmatrix}, \tag{13}$$

where the matrices $\mathbf{E}_a(M_\infty)$, $\mathbf{A}_a(M_\infty)$ and $\mathbf{C}_a(M_\infty)$ have been obtained in Eq. 7. In a more compact notation:

$$\mathbf{E}_{ae}(M_\infty)\frac{d\mathbf{x}_{ae}}{dt} = \mathbf{A}_{ae}(M_\infty)\mathbf{x}_{ae},$$

where $\mathbf{E}_{ae}(M_\infty) \in \mathbb{R}^{(2n_h+n_a)\times(2n_h+n_a)}$ and $\mathbf{A}_{ae}(M_\infty) \in \mathbb{R}^{(2n_h+n_a)\times(2n_h+n_a)}$. The stability of the aeroelastic system can now be analyzed by solving a generalized eigenvalue problem with generalized eigenvalue λ and generalized eigenvector $\boldsymbol{\phi}$:

$$(\lambda\mathbf{E}_{ae}(M_\infty) - \mathbf{A}_{ae}(M_\infty))\boldsymbol{\phi} = \mathbf{0}, \tag{14}$$

which standard solution can be efficiently obtained by application of the generalized Schur decomposition (also known as QZ algorithm) for general nonsymmetric matrices and for the case where the matrix $\mathbf{E}_{ae}(M_\infty)$ is possibly singular (Moler and Stewart, 1973). This algorithm is implemented for instance in the function *eig* in MATLAB$^{\text{TM}}$. Note that due to the realness of the involved matrices $\mathbf{E}_{ae}(M_\infty)$ and $\mathbf{A}_{ae}(M_\infty)$, the number $2n_h + n_a$ of generalized eigenvalues will either be real or appear in complex conjugate pairs.

Compared to common flutter methods (such as the *p-k* and *g* formulations) carried out in the frequency-domain and resulting in a nonlinear eigenvalue problem, the proposed *p-L* method overcome previous limitations:

- A true damping representation, that is, a proper dependence of the GAF matrix $\mathbf{Q}_{hh}$ not only with the reduced frequency k but also with $g = Re\{p\}$ is achieved by the *p-L* method. This has been described in Section 2.1, as the Loewner realization in state-space form is able to represent the behavior for signals different than one-harmonic. This is also true for the *p* method, but in that case the GAF matrix is approximated by RFA techniques (Rodden and Bellinger, 1982, Burkhart, 1977, Abel, 1979), while within the *p-L* method the GAF matrix is exactly interpolated. Also, the *p-L* method does not require of an additional residualization of the high-frequency behavior as for time-domain simulations (Quero et al., 2019).

- All generalized eigenvalues of the aeroelastic system are found. As described by Van Zyl (2001), the solution of the nonlinear eigenvalue problem by the method of successive approximations may miss some of the eigenvalues if some conditions are not met. This can be

avoided by using a more general Newton-Raphson solver combined with the p-k of g methods (Cardani and Mantegazza, 1978) or by sweeping through the reduced frequency values as proposed by Van Zyl (2001) and implemented as the *PKS* method in companion form in MSC.Software (2011). Sweeping techniques require the solution of several linear eigenvalue problems in order to find the roots of the flutter equation. In the p-L method the generalized eigenvalue problem is solved only once, while the system matrices involved have a bigger size. Namely, the size of the square matrix $\mathbf{A}_{ae}\left(M_\infty\right)$ is $2n_h + n_a$, increased by the value n_a corresponding to the aerodynamic states. However, for all applications considered in Section 4, the solution of the generalized eigenvalue problem is more efficient than solving the complex nonlinear algebraic equation given by Eq. 12 with $2n_h + 2$ unknowns. Note that this nonlinear algebraic equation must be solved at least a number n_h of times in order to find the distinct roots corresponding to the wind-off frequencies.

- The roots corresponding to a divergence instability are also found by the p-L method. Note that in order to find the divergence roots by solving the nonlinear algebraic equation provided in Eq. 12, a number of solutions greater than n_h must be found, for which a convenient initial value must be provided. As stated by Edwards and Wieseman (2008), the presence of these additional roots is related to the non-constant coefficients in the nonlinear eigenvalue problem. Applications including the determination of divergence roots are considered in Section 4.1.2.

- Theoretically the p-L method should also be able to find the onset of instabilities of different nature, for example those triggered by the fluid mode. For instance, the reduction of the buffet onset in the transonic regime (Gao and Zhang, 2020) is given by the cross of an eigenvalue associated to a fluid mode pattern from the left-half complex plane with the imaginary axis. This effect has however not been investigated yet. In that case, the possible virtual unstable modes which may appear by applying the Loewner realization would have to be carefully distinguished from those physical fluid modes causing the onset of stability.

Table 1 summarizes some of the characteristics inherent to previous methods compared to the proposed p-L method. There, the p-k method refers to either of the formulations available, namely, the original due to Hassig (1971) or including the additional aerodynamic damping matrix (Rodden et al., 1979). Regarding the p method, the specific number of aerodynamic states n_a depends on the type of RFA used (Roger, 1977, Karpel, 1982, Morino et al., 1995, Pasinetti and Mantegazza, 1999, Ripepi and Mantegazza, 2013), which in general differs from the number of the aerodynamic states required by the p-L method. As a side note, the term "interpolated" when referring to the the aerodynamic GAF matrix $\mathbf{Q}_{hh}\left(ik, M_\infty\right)$ over the imaginary axis refers to the consideration of the values as obtained by the aerodynamic model. In order to distinguish it from the p method, where approximated values are used due to the fitting process, "interpolated" is used to refer to the fact that a finite set of frequency points are chosen over the imaginary axis. For mtehods different than the p and the p-L methods, a complex interpolation (for instance after splitting the real and imaginary parts) is performed on the GAF matrix for frequencies not considered in the aerodynamic solver.

3.2. Mode tracking

Upon the solution of the generalized eigenvalue problem defined in Eq. 14 a set of real and complex conjugate pairs of generalized eigenvalues is obtained. If the flutter stability due to structural dof is of interest, the subset of eigenvalues "corresponding" to the wind-off set of n_h

Flutter solution method	Aerodynamic term $\mathbf{Q}_{hh}\left(ik, M_\infty\right)$	True damping	Problem type	Iterative solution	Number of times to be solved	System size
p-k (Hassig, 1971, Rodden et al., 1979)	Interpolated	No	Nonlinear eigenvalue	Yes or sweep	$\geq n_h$	• Complex matrices: n_h • Companion form: $2n_h$ • Nonlinear solver: $2n_h + 2$
PKS (MSC.Software, 2011)	Interpolated	No	Nonlinear eigenvalue	Sweep	$\geq n_h$	As for the *p-k* method
g (Chen, 2000)	Interpolated	Approximated	Nonlinear eigenvalue	Yes or sweep	$\geq n_h$	• Complex matrices: n_h • Companion form: $2n_h$ • Nonlinear solver: $2n_h + 2$
p (Burkhart, 1977, Abel, 1979, Rodden and Bellinger, 1982)	Approximated	Yes	Standard eigenvalue	No	1	$2n_h + n_a$
GAAM (Cunningham and Desmarais, 1984, Edwards and Wieseman, 2008)	Interpolated	Yes	Nonlinear eigenvalue	Yes	$\geq n_h$	• Complex matrices: n_h • Companion form: $2n_h$ • Nonlinear solver: $2n_h + 2$
p-L	Interpolated	Yes	Generalized eigenvalue	No	1	$2n_h + n_a$

Table 1: Comparison of previous methods with the *p-L* method for the solution of the flutter stablity problem.

structural modes $\boldsymbol{\phi}_0$ can be selected. This is done by substituting the eigensolutions computed by the p-L method, Eq. 14, into the original flutter equation, Eq. 9, that is, $p = \lambda_j \left(L_{ref}/U_\infty \right),\ j = 1, ..., 2n_h + n_a$. For each solution the 2-norm of the product

$$\left\| \mathbf{F}_{hh} \left(p, M_\infty \right) \mathbf{u}_h \left(p \right) \right\|_2 = \left\| \left(\frac{1}{\left\| \boldsymbol{\phi}_j \right\|_\infty} \right) \mathbf{F}_{hh} \left(\lambda_j \left(L_{ref}/U_\infty \right), M_\infty \right) \boldsymbol{\phi}_j \mathbf{T}_h \right\|_2$$

is evaluated, where the matrix $\mathbf{T}_h$ selects the first n_h components of the corresponding eigenvector $\boldsymbol{\phi}_j$. By sorting this norm in ascending order for all eigensolutions of the generalized eigenvalue problem, the first n_h eigensolutions associated to the structural dof can be identified. Note that the p-L method is general and this reduction step is not necessary if other types of stability, as for example caused by fluid modes (Gao and Zhang, 2020), are of interest.

After the optional reduction in the number of eigensolutions of the generalized eigenvalue problem, a mode tracking algorithm is applied. In this work the one of (Van Zyl, 1993) has been used, by which two eigenvectors $\boldsymbol{\phi}_a, \boldsymbol{\phi}_b \in \mathbb{C}^{n_h}$ are compared with a dedicated scalar product defined as:

$$< \boldsymbol{\phi}_a, \boldsymbol{\phi}_b >= \frac{\sqrt{S_1^2 + S_2^2}}{\sqrt{\left(\sum_{m=1}^{n_h} \left| \phi_{a,m} \right|^2 \right) \left(\sum_{m=1}^{n_h} \left| \phi_{a,b} \right|^2 \right)}}, \tag{15}$$

where:

$$S_1 = \sum_{m=1}^{n_h} \mathrm{Re}\left\{ \phi_{a,m} \right\} \mathrm{Re}\left\{ \phi_{b,m} \right\} + \mathrm{Im}\left\{ \phi_{a,m} \right\} \mathrm{Im}\left\{ \phi_{b,m} \right\},$$

$$S_2 = \sum_{m=1}^{n_h} \mathrm{Re}\left\{ \phi_{a,m} \right\} \mathrm{Im}\left\{ \phi_{b,m} \right\} - \mathrm{Im}\left\{ \phi_{a,m} \right\} \mathrm{Re}\left\{ \phi_{b,m} \right\}.$$

Note that in the application of the scalar product defined in Eq. 15 only the first n_h components of the eigenvectors $\boldsymbol{\phi}_a, \boldsymbol{\phi}_b$ are involved. When some eigenvalue (associated to the structural dof) crosses the imaginary axis from the left-half complex plane, the flutter condition is reached.

4. Application cases

In this section several flutter benchmark cases are considered for validation of the p-L method. Section 4.1 includes a structural 2 dof, heave (positive down) and pitch (positive nose up), in incompressible unsteady flow. Cases from the literature are selected and a discussion on the improvements shown my the p-L method is presented. Section 4.2 considers the well-known weakened AGARD445.6 flutter benchmark case in transonic flow (Yates, 1987). In the sequel the real part of the aeroelastic roots g are shown scaled as $2g/k$, as it is commonly done when solving the flutter stability problem (Chen, 2000).

4.1. Airfoil

It is common for the two-dimensional flutter cases analyzed here to carry out an additional nondimensionalization of the aeroelastic formulation as provided in Eq. 8:

$$\begin{bmatrix} 1 & x_\theta \\ x_\theta & r_\theta^2 \end{bmatrix} \frac{d^2}{dt^2}\left(\begin{bmatrix} h\left(t\right)/L_{ref} \\ \theta\left(t\right) \end{bmatrix}\right) + \begin{bmatrix} g_s\omega_h & 0 \\ 0 & g_s r_\theta^2 \omega_\theta \end{bmatrix} \frac{d}{dt}\left(\begin{bmatrix} h\left(t\right)/L_{ref} \\ \theta\left(t\right) \end{bmatrix}\right)$$
$$+ \begin{bmatrix} \omega_h^2 & 0 \\ 0 & \left(r_\theta\omega_\theta\right)^2 \end{bmatrix} \begin{bmatrix} h\left(t\right)/L_{ref} \\ \theta\left(t\right) \end{bmatrix} = \frac{1}{\mu\pi}\left(\frac{U_\infty}{L_{ref}}\right)^2 \begin{bmatrix} -c_l\left(t\right) \\ 2c_m\left(t\right) \end{bmatrix},$$

with $x_\theta = e - a$ the nondimensional static unbalance, r_θ the nondimensional moment of inertia, g_s the structural modal damping and the wind-off bending and torsional frequencies are represented by ω_h and ω_θ in (rad/s). The nondimensional position of the center of gravity is given by $e \in [-1, 1]$, whereas the nondimensional location of the elastic axis is denoted by $a \in [-1, 1]$. The reference length L_{ref} is equal to the semichord $c/2$ and μ represents the mass ratio. The aerodynamic forces are represented by the lift and pitch moment (at the elastic axis location) coefficients c_l and c_m.

4.1.1. Theodorsen and Garrick

Here the results of Theodorsen and Garrick (1940) and revisited by Zeiler (2000) are considered. The nondimensional parameters defined in Section 4.1 are set to:

$$a = -0.3,\ g_s = 0,\ r_\theta = 0.5,\ \mu = 20.$$

Fig. 9 shows a comparison between the nondimensional flutter speed $U_F/\omega_\theta L_{ref}$ as obtained by Zeiler and the present *p-L* method for two values of the static unbalance x_θ. Note that due to the nondimensionalization of the flutter speed, the solution depends on the ratio ω_h/ω_θ. As expected, the same predictions are obtained. Fig. 10 shows the evolution of the real part of the roots of the flutter equation as obtained by the *p-k*, *g*, *p-L* and the GAAM (reference) methods for the case $x_\theta = 0.2$ and $\omega_h/\omega_\theta = 0.3$. As it can be observed, for mode 1 (corresponding to the heave motion) with a greater real part and thus further away from the imaginary axis, the *g* method improves the the *p-k* prediction for value of g around -1. For more negative values of the real part *g* the *g* method does not necessarily improve the *p-k* prediction, as it based on a first-order Taylor series expansion around the imaginary axis. Thus, for roots of the flutter equation far from the imaginary axis there is in principle no guarantee that the *g* method will improve this prediction. As expected, the *p-L* method shows the proper description when compared to the GAAM reference method for all values of *g*.

4.1.2. HA145A

Now the *p-L* method is applied to the two cases known as HA145A and considered by Rodden and Bellinger (1982), Chen (2000) and Van Zyl (2001). The nondimensional parameters of Section 4.1 are set to:

$$a = -0.2,\ g_s = 0.03,\ r_\theta = 0.5,\ \omega_h = 10\ (\text{rad/s}),\ \omega_\theta = 25\ (\text{rad/s}),\ \mu = 20.$$

Two different subcases are distinguished, namely, the HA145A1 case with $x_\theta = -0.06$ with a divergence speed U_D below the flutter speed U_F, and the HA145A2 case with $x_\theta = 0.1$ with a divergence speed U_D above the flutter speed U_F. As described in Section 3.1, the *p-L* method is able to obtain all roots of the aeroelastic system at once, including the divergence roots. Tables 2 and 3 show the flutter and divergence speeds obtained in different references compared to the *p-L* method. As expected, both flutter and divergence speeds are predicted by the *p-L* method.

The mode tracking algorithm of Section 3.2 was applied for the modes shown in Figs. 11 and 12, where the evolution of the scaled real part of the roots of the flutter equation $2g/k$ are plotted

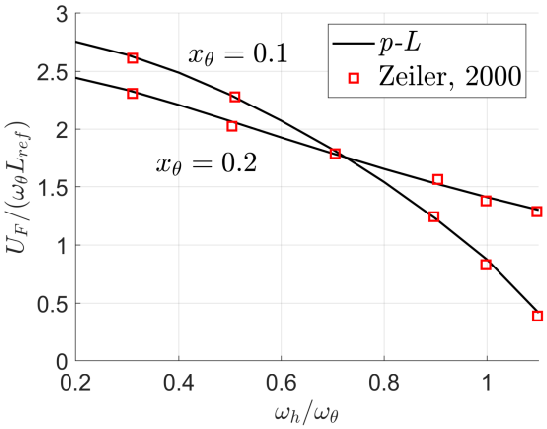

Figure 9: Nondimensional flutter speed $U_F/\omega_\theta L_{ref}$ as obtained by Zeiler (2000) and the p-L method.

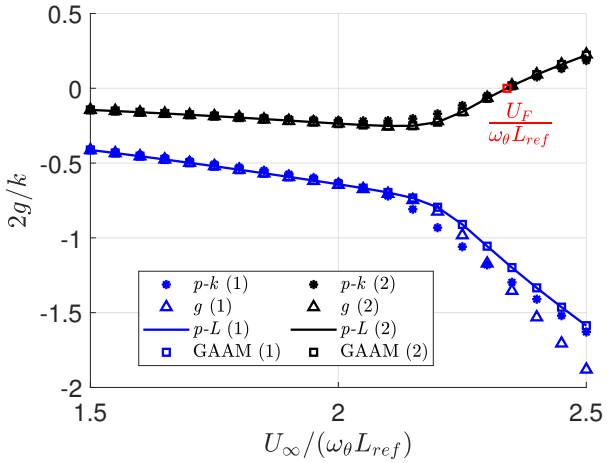

Figure 10: Scaled real part of the roots $2g/k$ of the flutter equation versus the nondimensional speed $U_\infty/\omega_\theta L_{ref}$ with $x_\theta = 0.2$ and $\omega_h/\omega_\theta = 0.3$.

Source	Divergence speed U_D (m/s)	Flutter speed U_F (m/s)
Chen Chen (2000)	64.0080	76.2000
Van Zyl Van Zyl (2001)	65.9892	77.1144
p-L method	65.9009	76.8502

Table 2: Divergence and flutter speeds for the HA145A1 benchmark case.

Source	Divergence speed U_D (m/s)	Flutter speed U_F (m/s)
Chen Chen (2000)	68.5800	51.8160
p-L method	65.7624	51.0816

Table 3: Divergence and flutter speeds for the HA145A2 benchmark case.

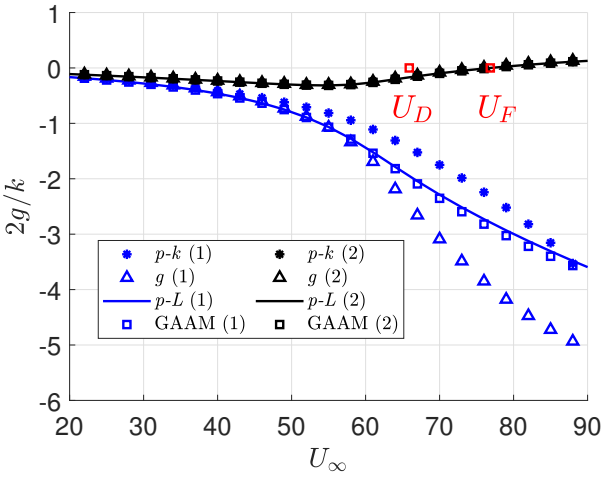

Figure 11: Scaled real part of the roots of the flutter equation $2g/k$ versus the true airspeed U_∞. Case HA145A1 with $x_\theta = -0.06$.

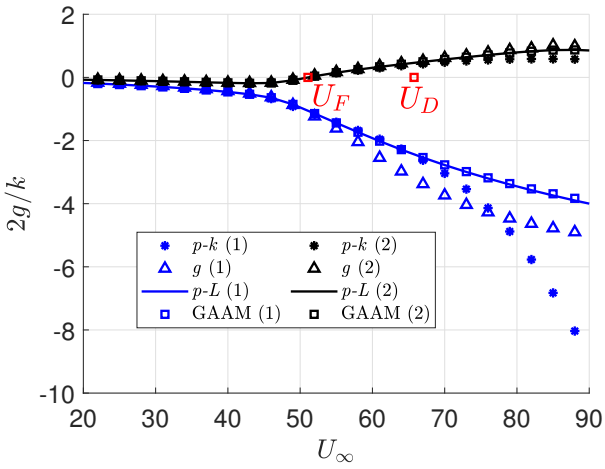

Figure 12: Real part of the roots of the flutter equation $2g/k$ versus the true airspeed U_∞. Case HA145A2 with $x_\theta = 0.1$.

against the true airspeed U_∞. For the identification of the divergence root, the root of the flutter equation with minimum real part $\min(|g|)$ was identified. When this root crossed the imaginary axis, the divergence speed U_D is reached.

Similarly to the conclusions drawn in Section 4.1.1, the *p-L* method is able to improve the predictions of the *g* method, matching the predictions of GAAM method and representing thus a true damping solution to the flutter equation for non pure one-harmonic cases.

4.2. Weakened AGARD 445.6 wing

The AGARD 445.6 wing is a widely used aeroelastic benchmark problem (Yates, 1987). This 45 (deg) swept-back wing with an aspect ratio of 1.65 has been tested at the NASA Langley Transonic Dynamics Tunnel (TDT). The wing has no twist and the thin NACA64A004 airfoil is symmetric. The structural characteristics of the wing are provided in the form of measured natural frequencies and mode shapes derived from a finite element model, and its flutter characteristics have been studied experimentally (Yates, 1987). Here the weakened version of the wing is considered, for which experimental data in a range of Mach numbers are available.

As discussed by Silva et al. (2014), due to the thin airfoil, the transonic regime is limited to Mach numbers very close to 1 and thus linear aerodynamic theories which account for compressibility may be used for the prediction of its flutter characteristics. In this work a its aerodynamic characteristics have been computed with potential DLM solver (MSC.Software, 2011) for an isolated wing with 144 panels and a vertical symmetry plane at the root. For the transfer of forces and displacement between the aerodynamic and computational meshes a thin plate spline (TPS) (Duchon, 1977) has been used. Experimental flutter results for cases testes in air and Mach number below 1 are presented in Table 4. The subscript F refers to the flutter condition and has been added in order to match the process used for the determination of the flutter condition with the computations method. Indeed, in order to determine numerically the flutter condition, fixed values of the Mach number M_∞ and airspeed U_∞ for each test point are kept and the dynamic pressure is progressively increased from 2000 (Pa) in intervals of 1000 (Pa) with a corresponding increased in density. The condition at which a real part of any root of the flutter equation becomes zero (from the negative

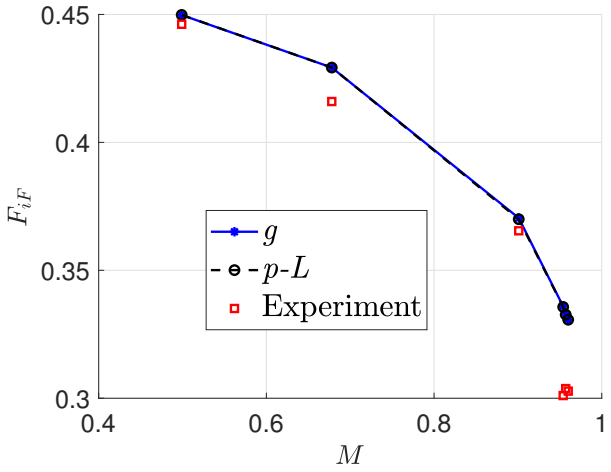

Figure 13: Nondimensional flutter speed index F_{iF} for different test points. AGARD 445.6 wing.

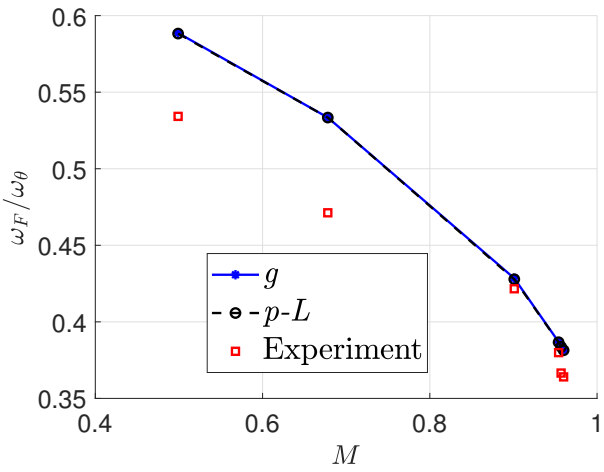

Figure 14: Nondimensional flutter frequency ω_F/ω_θ for different test points. AGARD 445.6 wing.

values), the flutter condition given by the dynamic pressure $q_{dyn,F}$ (or equivalently a density ρ_F) is met.

M_∞	U_∞ (m/s)	ρ_F (kg/m^3)	$q_{dyn,F}$ (Pa)	ω_F (rad/s)
0.499	172.4558	0.4278	6372.8626	128.1
0.678	231.3737	0.2082	5539.7461	113.0
0.901	296.6923	0.0995	4275.7072	101.1
0.954	307.3603	0.0634	2901.5438	91.1
0.957	310.9570	0.0634	2954.2120	87.9
0.960	309.0062	0.0634	2935.0599	87.3

Table 4: Experimental test points for AGARD 445.6 weakened wing.

Figs. 13 and 14 show a comparison of the experimental flutter data with the obtained flutter conditions determined by the g and p-L methods. The flutter speed index is defined as $F_{iF} = U_F/\left(L_{ref}\omega_\theta\sqrt{\mu}\right)$ with U_F the flutter speed and the frequency at the flutter condition ω_F has been nondimensionalized with the torsional wind-off frequency ω_θ. The reference length is $L_{ref} = 0.2789$ (m). As expected, both methods deliver the same results, but with the p-L method solving a generalized eigenvalue problem instead of a nonlinear eigenvalue problem. For the determination of the flutter roots for one particular combination of Mach number, airspeed and dynamic pressure (or density), the p-L method requires in this case 1/2 of the computational time needed by the p-k method and 1/4 of the computational time required by the g method, including the building of the aerodynamic matrices in Eq. 7. Note that a higher computational time is required by the g method when compared to the p-k method in order to determine the additional derivative term $d\mathbf{Q}_{hh}\left(ik, M_\infty\right)/d\left(ik\right)$ in Eq. 1 by finite differences.

Additionally to the computational advantage and the fact that all roots to the flutter equation are found (see Section 3.1), the p-L method determines the flutter roots with a true damping component. Figs. 15 and 16 show the evolution of the flutter roots (real and imaginary parts k and g respectively) with respect to the speed index $F_i = U_\infty/\left(L_{ref}\omega_\theta\sqrt{\mu}\right)$. Both the g method and p-L methods coincide in this case, indicating that in this case the perturbation g method is

able to predict the damping. The p-L method is not subjected to the restriction of small damping values and thus it is also valid for higher damping values.

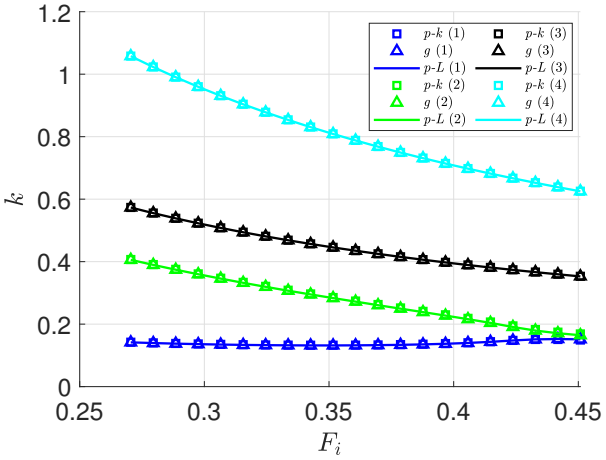

Figure 15: Reduced frequency of aeroelastic modes at test point $M_\infty = 0.678$ and $\rho_\infty = 0.2082$ (kg/m^3). AGARD 445.6 wing.

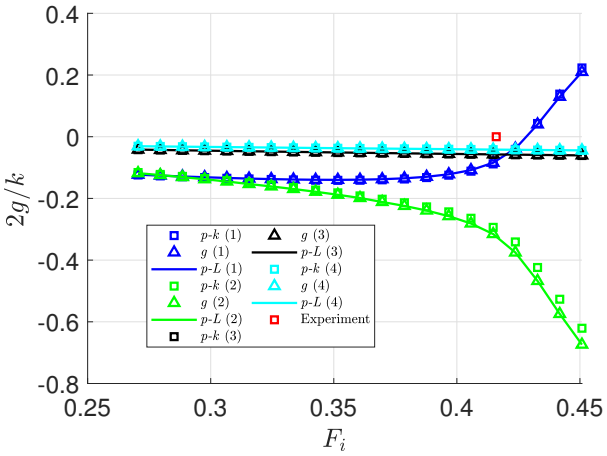

Figure 16: Scaled damping of aeroelastic modes ($2g/k$) at test point $M_\infty = 0.678$ and $\rho_\infty = 0.2082$ (kg/m^3) and experimental flutter speed index. AGARD 445.6 wing.

5. Conclusions

In this work a novel flutter solution method denoted as the p-L method has been presented. It overcomes limitations inherent to existing flutter solution methods in that it truly represents the damping term and avoids an iterative nonlinear solution in order to determine the roots of the determinant of the flutter equation. This is done by transforming the nonlinear aerodynamic term into a generalized state-space form which represents a truly interpolation throughout the complex plane. In contrast to the existing p method, the nonlinear term is interpolated and not approximated, avoiding the incursion of approximation errors.

The p-L method relies on the solution of a standard eigenvalue problem and thus computes all roots simultaneously. Additional roots as in the case of aeroelastic divergence are also obtained. The roots of the determinant of the flutter equation can be sorted afterwards according to a mode tracking algorithm, which is in turn applied as a post-processing step and as such does not affect the solution algorithm. Several flutter benchmark cases have been selected for the demonstration of the p-L method, achieving a true damping representation as for the GAAM method but avoiding the computation of the aerodynamic term outside the imaginary axis. Also, all roots are obtained at once avoiding the possible loss of roots, which may happen when using iterative methods or a nonlinear algebraic solver, as required for the GAAM method.

The stability analysis presented in this work has been focused on instabilities involving the structural generalized coordinates, namely, flutter and divergence. However, the p-L method presented here is more general and the prediction of instabilities caused for instance by a fluid mode are left for future work.

References

Abel, I., 1979. An analytical technique for predicting the characteristics of a flexible wing equipped with an active flutter-suppression system and comparison with wind-tunnel data. NASA Technical Paper 1367 .

Albano, E., Rodden, W., 1969. A doublet-lattice method for calculating lift distributions on oscillating surfaces in subsonic flows. AIAA Journal 7, 279–285. https://doi.org/10.2514/3.5086.

Anon., 2018. Certification specifications for large aeroplanes (CS-25), amendment 21, European Aviation Safety Agency (EASA) , 229–231.

Bindolino, G., Mantegazza, P., 1987. Aeroelastic derivatives as a sensitivity analysis of nonlinear equations. AIAA Journal 25, 1145–1146. https://doi.org/10.2514/3.9758.

Burkhart, T., 1977. Subsonic transient lifting surface aerodynamics. Journal of Aircraft 14, 44–50. https://doi.org/10.2514/3.58748.

Cardani, C., Mantegazza, P., 1978. Continuation and direct solution of the flutter equation. Computers and Structures 8, 185 – 192. https://doi.org/10.1016/0045-7949(78)90021-4.

Carrier, G., Krook, M., Pearson, C., 2005. Functions of a complex variable: theory and technique. SIAM.

Chen, P., 2000. Damping perturbation method for flutter solution: The g-method. AIAA Journal 38, 1519–1524. https://doi.org/10.2514/2.1171.

Cunningham, H., Desmarais, R., 1984. Generalization of the subsonic kernel function in the s-plane, with applications to flutter analysis. NASA Technical Paper 2292 .

Duchon, J., 1977. Splines minimizing rotation-invariant semi-norms in Sobolev spaces, in: Schempp, W., Zeller, K. (Eds.), Constructive Theory of Functions of Several Variables, Springer Berlin Heidelberg. pp. 85–100. https://doi.org/10.1007/BFb0086566.

Edwards, J., 1977. Unsteady aerodynamic modeling and active aeroelastic control. Ph.D. thesis. Stanford University.

Edwards, J., Ashley, H., Breakwell, J., 1979. Unsteady aerodynamic modeling for arbitrary motions. AIAA Journal 17, 365–374. https://doi.org/10.2514/3.7348.

Edwards, J., Wieseman, C., 2008. Flutter and divergence analysis using the generalized aeroelastic analysis method. Journal of Aircraft 45, 906–915. https://doi.org/10.2514/1.30078.

Gao, C., Zhang, W., 2020. Transonic aeroelasticity: A new perspective from the fluid mode. Progress in Aerospace Sciences 113, 100596. https://doi.org/10.1016/j.paerosci.2019.100596.

Gosea, I., Zhang, Q., Antoulas, A., 2020. Preserving the DAE structure in the Loewner model reduction and identification framework. Advances in Computational Mathematics 46, 3. https://doi.org/10.1007/s10444-020-09752-8.

Haddadpour, H., Firouz-Abadi, R., 2009. True damping and frequency prediction for aeroelastic systems: The PP method. Journal of Fluids and Structures 25, 1177 – 1188. https://doi.org/10.1016/j.jfluidstructs.2009.06.006.

Hassig, H., 1971. An approximate true damping solution of the flutter equation by determinant iteration. Journal of Aircraft 8, 885–889. https://doi.org/10.2514/3.44311.

Ionita, A., 2013. Lagrange rational interpolation and its applications to approximation of large-scale dynamical systems. Ph.D. thesis. Rice University.

Jacobson, K., Stanford, B., Wood, S., Anderson, W.K., 2020. Flutter analysis with stabilized finite elements based on the linearized frequency-domain approach. AIAA Scitech Forum https://doi.org/10.2514/6.2020-0403. https://arc.aiaa.org/doi/pdf/10.2514/6.2020-0403.

Ju, Q., Qi, S., 2009. New improved g method for flutter solution. Journal of Aircraft 46, 2184–2186. https://doi.org/10.2514/1.46328.

Karpel, M., 1982. Design for active flutter suppression and gust alleviation using state-space aeroelastic modeling. Journal of Aircraft 19, 221–227. https://doi.org/10.2514/3.57379.

Khalil, H., Grizzle, J., 2002. Nonlinear systems. volume 3. Prentice hall Upper Saddle River, NJ.

Marques, A., Azevedo, J., 2008. Numerical calculation of impulsive and indicial aerodynamic responses using computational aerodynamics techniques. Journal of Aircraft 45, 1112–1135. https://doi.org/10.2514/1.32151.

Mayo, A., Antoulas, A., 2007. A framework for the solution of the generalized realization problem. Linear algebra and its applications 425, 634–662. https://doi.org/10.1016/j.laa.2007.03.008.

Moler, C., Stewart, G., 1973. An algorithm for generalized matrix eigenvalue problems. SIAM Journal on Numerical Analysis 10, 241–256. https://doi.org/10.1137/0710024.

Morino, L., Mastroddi, F., Troia, R.D., Ghiringhelli, G.L., Mantegazza, P., 1995. Matrix fraction approach for finite-state aerodynamic modeling. AIAA Journal 33, 703–711. https://doi.org/10.2514/3.12381.

MSC.Software, 2011. MSC.Nastran 2012 quick reference guide .

Pasinetti, G., Mantegazza, P., 1999. Single finite states modeling of aerodynamic forces related to structural motions and gusts. AIAA Journal 37, 604–612. https://doi.org/10.2514/2.760.

Pitt, D., 1999. A new non-iterative p-k match point flutter solution. 40th Structures, Structural Dynamics, and Materials Conference and Exhibit https://doi.org/10.2514/6.1999-1353. https://arc.aiaa.org/doi/pdf/10.2514/6.1999-1353.

Powell, M., 1968. A Fortran subroutine for solving systems of nonlinear algebraic equations. Technical Report AERE-R-5947.

Quero, D., Vuillemin, P., Poussot-Vassal, C., 2019. A generalized state-space aeroservoelastic model based on tangential interpolation. Aerospace 6, 9. https://doi.org/10.3390/aerospace6010009.

Ripepi, M., Mantegazza, P., 2013. Improved matrix fraction approximation of aerodynamic transfer matrices. AIAA Journal 51, 1156–1173. https://doi.org/10.2514/1.J052009.

Rodden, W., Bellinger, E., 1982. Aerodynamic lag functions, divergence, and the british flutter method. Journal of Aircraft 19, 596–598. https://doi.org/10.2514/3.44772.

Rodden, W., Harder, R., Bellinger, E., 1979. Aeroelastic addition to NASTRAN. NASA Contractor Report 3094 .

Roger, K.L., 1977. Airplane math modeling methods for active control design. AGARD-CP-228 , 4.1–4.11.

Shinners, S., 1998. Modern control system theory and design. John Wiley & Sons.

Silva, W., Chwalowski, P., Perry III, B., 2014. Evaluation of linear, inviscid, viscous, and reduced-order modelling aeroelastic solutions of the AGARD 445.6 wing using root locus analysis. International Journal of Computational Fluid Dynamics 28, 122–139. https://doi.org/10.1080/10618562.2014.922179.

Stark, V., 1984. General equations of motion for an elastic wing and method of solution. AIAA Journal 22, 1146–1153. https://doi.org/10.2514/3.8750.

Theodorsen, T., 1935. General theory of aerodynamic instability and the mechanism of flutter. NACA Technical Report 496 .

Theodorsen, T., Garrick, I., 1940. Mechanism of flutter: a theoretical and experimental investigation of the flutter problem. NACA Technical Report 685 .

Thormann, R., Widhalm, M., 2013. Linear-frequency-domain predictions of dynamic-response data for viscous transonic flows. AIAA Journal 51, 2540–2557. https://doi.org/10.2514/1.J051896.

Trefethen, L., 2019. Approximation theory and approximation practice. SIAM.

Trefethen, L., 2020. Quantifying the ill-conditioning of analytic continuation. BIT Numerical Mathematics , 1–15https://doi.org/10.1007/s10543-020-00802-7.

Van Zyl, L., 1993. Use of eigenvectors in the solution of the flutter equation. Journal of Aircraft 30, 553–554. https://doi.org/10.2514/3.46380.

Van Zyl, L., 2001. Aeroelastic divergence and aerodynamic lag roots. Journal of Aircraft 38, 586–588. https://doi.org/10.2514/2.2806.

Wang, Y., Lei, C., Pang, G., Wong, N., 2010. MFTI: Matrix-format tangential interpolation for modeling multi-port systems. Design Automation Conference , 683–686.

Yates, E., 1987. Agard standard aeroelastic configurations for dynamic response. Candidate configuration I.-wing 445.6. AGARD Report No.765 .

Zeiler, T., 2000. Results of Theodorsen and Garrick revisited. Journal of Aircraft 37, 918–920. https://doi.org/10.2514/2.2691.